SYMPOSIUM REVIEW

Ivermectin and its target molecules: shared and unique modulation mechanisms of ion channels and receptors by ivermectin

I-Shan Chen[1,2] iD and Yoshihiro Kubo[1,2]

[1]*Division of Biophysics and Neurobiology, Department of Molecular and Cellular Physiology, National Institute for Physiological Sciences, Okazaki 444-8585, Japan*
[2]*Department of Physiological Sciences, School of Life Science, SOKENDAI (The Graduate University for Advanced Studies), Hayama 240-0193, Japan*

Edited by: Ole Petersen & David Adams
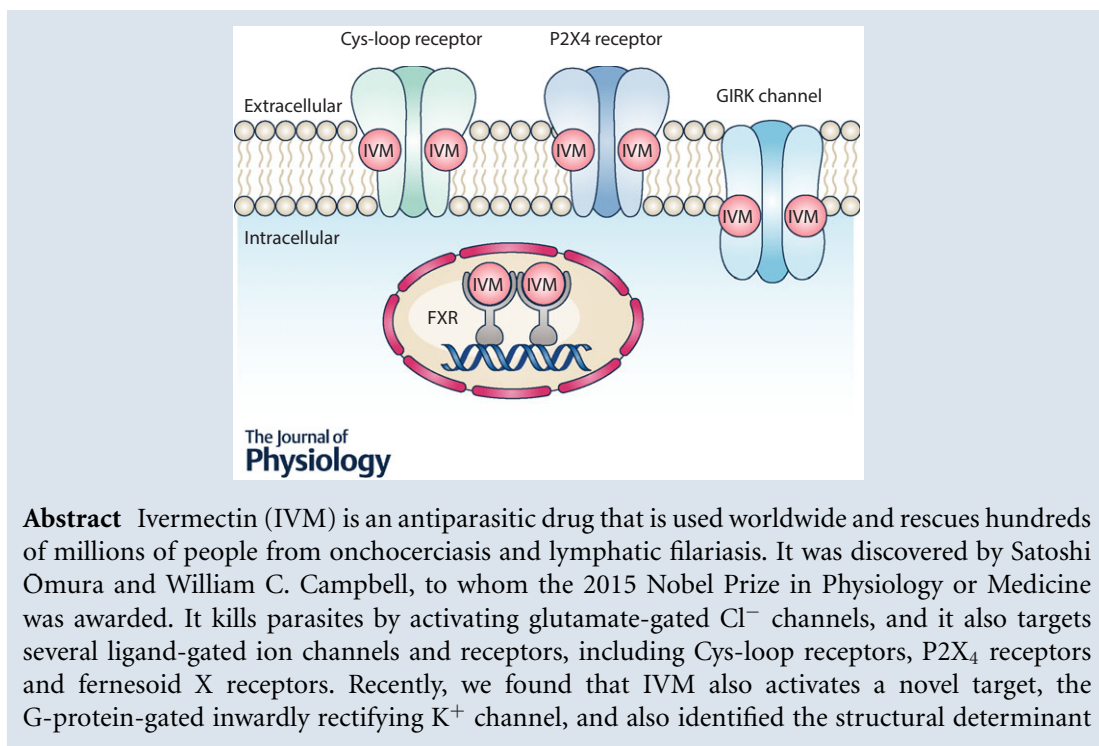
Abstract Ivermectin (IVM) is an antiparasitic drug that is used worldwide and rescues hundreds of millions of people from onchocerciasis and lymphatic filariasis. It was discovered by Satoshi Omura and William C. Campbell, to whom the 2015 Nobel Prize in Physiology or Medicine was awarded. It kills parasites by activating glutamate-gated Cl^- channels, and it also targets several ligand-gated ion channels and receptors, including Cys-loop receptors, $P2X_4$ receptors and fernesoid X receptors. Recently, we found that IVM also activates a novel target, the G-protein-gated inwardly rectifying K^+ channel, and also identified the structural determinant

I-Shan Chen received her PhD from Osaka University (where her supervisor was Prof. Yoshihisa Kurachi) where she started the GPCR–GIRK studies. After performing post-doctoral research in the same laboratory, she moved to the National Institute for Physiological Sciences as an assistant professor (where her principal investigator (PI) is Prof. Yoshihiro Kubo) in 2015. **Yoshihiro Kubo** received his PhD from The University of Tokyo (where his supervisor was the late Prof. Kunitaro Takahashi) and performed post-doctoral research in University of California San Francisco (where his PI was Prof. Lily Jan). He engaged in structure–function studies of membrane proteins in Tokyo Metropolitan Institute for Neurosciences and then in Tokyo Medical and Dental University. He has been a professor of the National Institute for Physiological Sciences since 2003.
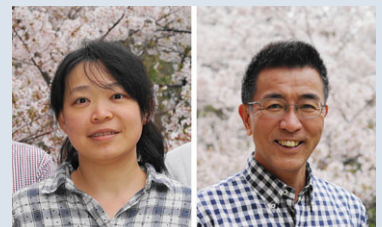
This review was presented at the symposium 'Shared and unique aspects of the gating mechanisms of ligand- and voltage-gated ion channels' which took place at IUPS 38th World Congress, Rio de Janeiro, Brazil, 1–5 August 2017.

for the activation. In this review, we aim to provide an update and summary of recent progress in the identification of IVM targets, as well as their modulation mechanisms, through molecular structures, chimeras and site-directed mutagenesis, and molecular docking and modelling studies.

Abstract figure legend The IVM-binding site in Cys-loop receptors and the farnesoid X receptor (FXR), and the predicted IVM-binding site in the P2X$_4$ receptor and the G-protein-gated inwardly rectifying K$^+$ (GIRK) channel.

Introduction

Ivermectin (IVM) is a well-known antiparasitic drug that rescues humans and domestic animals from parasitic infection such as onchocerciasis (river blindness) and lymphatic filariasis. In the 1970s, Satoshi Ōmura isolated a mixture that consists of eight components (A1a, A1b, A2a, A2b, B1a, B1b, B2a and B2b) from *Streptomyces avermitilis*. Then, he and his collaborator, William C. Campbell, identified several 16-membered macrocyclic lactone derivatives (known as avermectins), which possess high anthelmintic activity that kills parasitic worms (Burg *et al.* 1979; Egerton *et al.* 1979). IVM is one of the avermectins and consists of a mixture of B1a and B1b components in an 80:20 ratio (Fig. 1). In the 1980s, IVM became a commercially available drug, since it was found to be safer and more potent than other avermectins (Chabala *et al.* 1980; Campbell *et al.* 1983; Campbell & Benz, 1984). To date, IVM has contributed to the improvement of the health of hundreds of millions of people in many developing communities and in consequence has been included on the Model List of Essential Medicines of the World Health Organization (Omura, 2016).

IVM is highly hydrophobic and deeply inserts into the subunit interfaces of transmembrane domains (TMs) of Cys-loop receptor family members (Lynagh & Lynch, 2012). When IVM binds to the glutamate-gated Cl$^-$ channel (GluCl), a member of the Cys-loop receptor family found in invertebrates, it potentiates the channel activity, resulting in hyperpolarization of parasite neurons and muscles, thereby killing the parasites (Cully *et al.* 1994; Arena *et al.* 1995). Mutations in GluCl reduce IVM sensitivity and thereby produce IVM resistance in parasites and insects (Kane *et al.* 2000; McCavera *et al.* 2009; Ghosh *et al.* 2012). IVM also interacts with the TMs of other Cys-loop receptors, including the histamine-gated Cl$^-$ channel (Zheng *et al.* 2002), the pH-gated Cl$^-$ channel (Mounsey *et al.* 2007; Nakatani *et al.* 2016), the glycine receptor (GlyR) (Shan *et al.* 2001), the γ-aminobutyric acid receptor (GABA$_A$R) (Adelsberger *et al.* 2000) and the α7-nicotinic acetylcholine receptor (nAChR) (Krause *et al.* 1998). IVM also modulates the P2X$_4$ receptor and most likely binds to the TMs of this receptor, similarly to

the Cys-loop receptors described above (Silberberg *et al.* 2007).

The farnesoid X receptor (FXR), a nuclear receptor involved in metabolic regulation, is also a novel target of IVM (Jin *et al.* 2013). Also, it was reported that IVM acts as an inhibitor of the human *ether-à-go-go*-related gene (hERG) K$^+$ channel with an IC$_{50}$ of approximately 13 μM at 23°C and 24 μM at 37°C (Kauthale *et al.* 2015).

We recently revealed that IVM activates a novel target, the G-protein-gated inwardly rectifying K$^+$ (GIRK) channel, especially subtype 2 (GIRK2) (Chen *et al.* 2017). In remarkable contrast to the critical site for IVM binding in Cys-loop receptors and the P2X$_4$ receptor, we found that the interface between the TMs and intracellular domains, rather than the TMs themselves, plays critical roles in IVM-induced GIRK activation. Here we introduce novel information as to how IVM modulates ion channels and receptors, by summarizing the findings from structural and functional points of view.

Roles of IVM and the structural determinants for the modulation of targets

Cys-loop receptors. IVM acts as an activator or modulator of Cys-loop receptors, including invertebrate GluCl and human inhibitory anion-permeable receptors (GlyR and GABA$_A$R) and an excitatory cation-permeable receptor (nAChR). Another human cation-permeable Cys-loop receptor, the type 3 5-hydroxytryptamine receptor (5-HT$_3$R), is insensitive to IVM. These Cys-loop receptors have a similar structure but are activated by different neurotransmitters, such as glycine, glutamate, acetylcholine and serotonin, while controlling excitatory or inhibitory synaptic transmission in the central nervous system.

In recent years, high resolution structures of several Cys-loop receptors have been solved by X-ray crystallography or cryo-electron microscopy: GluCl (Hibbs & Gouaux, 2011), GABA$_A$R (Miller & Aricescu, 2014), GlyR (Du *et al.* 2015; Huang *et al.* 2017) and nAChR (Unwin, 2005; Morales-Perez *et al.* 2016). In general, Cys-loop receptors are pentamers of the same or different subunits, in which each subunit contains an N-terminal extracellular

domain and four TMs, and the TM2 helices from each subunit line the channel pore. The Cys-loop is one of the domains that connect the extracellular domains and the TMs. When a neurotransmitter binds to the pocket in the extracellular domain, conformational changes are transmitted to the TMs to open the channel pore. There are only two of the Cys-loop receptor family members whose structures have been solved in an IVM-bound complex: *Caenorhabditis elegans* GluCl (Hibbs & Gouaux, 2011) and the zebrafish and human GlyRs (Du *et al.* 2015; Huang *et al.* 2017) (Fig. 2*A*). The IVM-bound structures of other IVM-targeted Cys-loop receptors remain unknown.

In the case of GluCl, IVM acts as an activator with an EC_{50} of 140 nM or an allosteric modulator at a low concentration (5 nM) that potentiates glutamate binding (Cully *et al.* 1994). IVM binds to the TMs at the subunit interface of the GluCl pentamer, near the extracellular surface of the plasma membrane (Hibbs & Gouaux, 2011) (Fig. 2*A*, left panel). By comparing the structures between an apo (closed) state and an IVM-bound (open) state of GluCl, the insertion of IVM is shown to enlarge the channel pore of the TM region (Hibbs & Gouaux, 2011; Althoff *et al.* 2014) (Fig. 2*B* and *C*). In the apo (closed) state, the side chain of Leu254, located in the narrowest position in the channel pore, acts as a closed gate. Althoff *et al* (2014) described that the activation of GluCl by

IVM induces a rotation and a shift of the TMs toward the extracellular side (an upward movement of the TMs), thereby enlarging the pore gate formed by Leu254 and also expanding the space in the inter-subunit interface between the TM1 and the TM3 helices (Althoff *et al.* 2014). Leu218 in TM1, Ser260 in TM2 and Thr285 in TM3 interact with IVM by forming hydrogen bonds (Fig. 2*D*). Gly281 in TM3 also contributes to IVM sensitivity (Lynagh & Lynch, 2010*a*). IVM binding stabilizes the TMs in an open state through an interaction between Pro268 and Val45 located at the interface between the extracellular domains and TMs (Calimet *et al.* 2013; Althoff *et al.* 2014). Conformational changes in the TMs by IVM also induce a tilt of the extracellular domain, which may potentiate the binding of glutamate.

In the case of GlyR, IVM acts as an activator at high concentrations, with an EC_{50} between 1 and 5 μM toward different GlyR subunits (Lynagh & Lynch, 2010*b*). IVM also acts as an allosteric modulator that potentiates the glycine (saturating concentration, 250 μM)-induced current at a low concentration (30 nM) (Shan *et al.* 2001). The IVM-binding site in GlyR is similar to that in GluCl (Fig. 2*A*, right panel). IVM also binds to the TMs at each subunit interface of the zebrafish GlyRα1 and human GlyRα3 pentamer, near the extracellular surface of the membrane (Du *et al.* 2015; Huang *et al.*

Component B1a: R = CH$_2$CH$_3$

Component B1b: R = CH$_2$CH$_3$

MW: 875
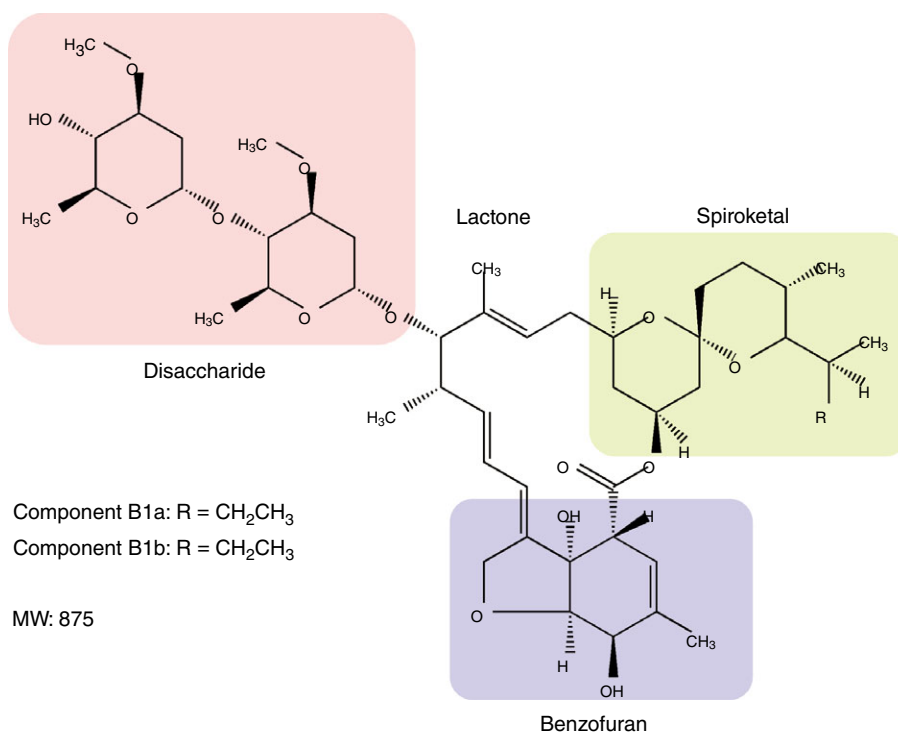
Figure 1. Chemical structure of IVM
IVM is a 16-membered macrocyclic lactone derivative with disaccharide, benzofuran and spiroketal moieties, and the molar mass is about 875 g mol^{-1}. It is a complex of 80% B1a and 20% B1b components. Previous studies suggested that the benzofuran moiety plays the most critical role in its interaction with GluCl (Michael *et al.* 2001; Lynagh & Lynch, 2012).
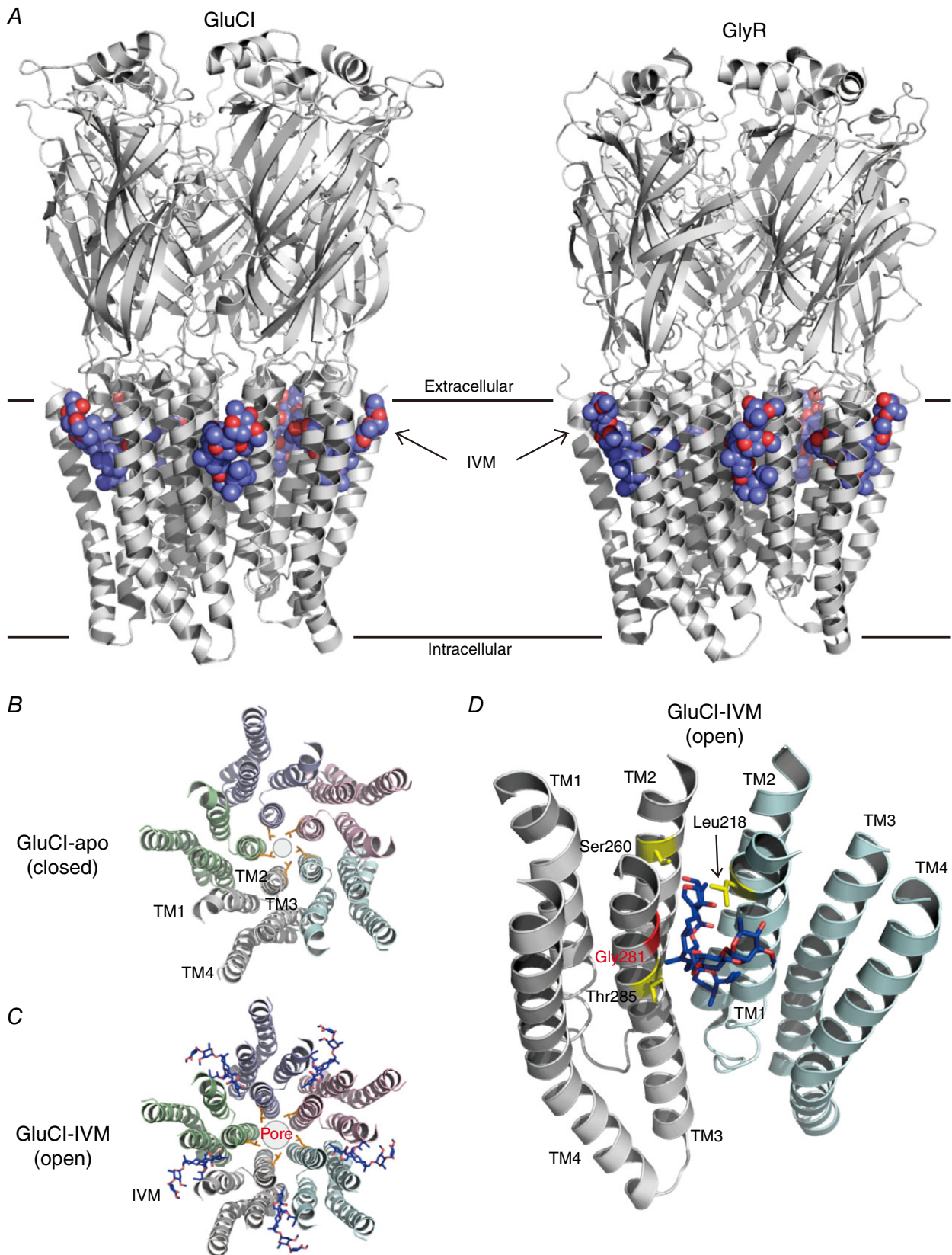
Figure 2. IVM binding site and its structural determinants in GluCl and GlyR

A, a lateral view (parallel to plasma membrane) of the structure of IVM-bound *C. elegans* GluCl (left panel; PDB ID: 3RHW) (Hibbs & Gouaux, 2011) and zebrafish GlyR (right panel; PDB ID: 3JAF) (Du *et al.* 2015) pentamer. The IVM molecules are shown in sphere mode. *B* and *C*, a top view (perpendicular to plasma membrane) of TMs of GluCl from the extracellular side in an apo (closed) state (*B*; PDB ID: 4TNV) (Althoff *et al.* 2014) and an IVM-bound (open) state (*C*; PDB ID: 3RHW). Each subunit is shown in a different colour and the shut gate of the channel pore, formed by the side chains of Leu254 in TM2 from each subunit, is shown in orange. The IVM molecules are shown in stick mode. The binding of IVM to GluCl enlarges the channel pore. *D*, IVM inserts into the subunit interface and interacts with Leu218 in TM1, Ser260 in TM2 and Thr285 in TM3 (shown in yellow) by forming hydrogen bonds. A key amino acid residue for IVM sensitivity in the Cys-loop receptor family (Gly281 in GluCl) is shown in red.

2017). In human GlyRα3, Pro230 in TM1 and Ala288 in TM3 (corresponding to Gly281 in GluCl) interact with IVM by forming hydrophobic interactions (Huang *et al.* 2017). The Ala288Gly mutation in GlyR increased IVM activity, suggesting that a smaller residue at this position gives a higher IVM sensitivity (Lynagh & Lynch, 2010*b*). Any residues larger than Gly at this corresponding position in Cys-loop receptors disturbs IVM binding, and this may be one of the reasons why IVM activates GlyR less potently than GluCl (IVM activates GlyR at a micromolar concentration and activates GluCl at a nanomolar concentration) (Lynagh & Lynch, 2010*a*, 2012; Huang *et al.* 2017). Ile225 and Gln226 in TM1 and Ser267 and Arg287 in TM2 of human GlyRα3 interact with IVM by forming hydrogen bonds (Huang *et al.* 2017). All of these residues contribute to IVM binding and sensitivity. By comparing the structures of the strychnine-bound (closed) state, glycine-bound (open) state and glycine–IVM-bound state of zebrafish GlyR, it was shown that there are two pore gates formed by Leu277 and Pro266 (Du *et al.* 2015). The insertion of IVM induces rotation of TMs and thus enlargement of the pore gate formed by Leu277 but constriction of the pore gate formed by Pro266 in TM2 (Du *et al.* 2015). Unlike in GluCl, the binding of IVM to glycine-bound GlyR induces remarkable conformational changes in TMs but only limited changes in the extracellular domains.

In the case of GABA$_A$R, the X-ray structure of the human GABA$_A$R β3 homopentamer revealed the agonist (benzamidine)-binding pocket in the extracellular domains (Miller & Aricescu, 2014), whereas the IVM-bound structure still remains unsolved. GABA$_A$Rs are usually composed of multiple kinds of subunits, and the major isoform in brain is composed of α1, β2 and γ2 subunits (Sigel & Steinmann, 2012). IVM activates the α1β2γ2 GABA$_A$R with an EC$_{50}$ of approximately 2−7 μM (Adelsberger *et al.* 2000; Westergard *et al.* 2015) and potentiates the native GABA-induced Cl$^-$ current in mouse hippocampal neurons at a low concentration (0.1 μM) (Zemkova *et al.* 2014). Based on functional studies and docking analyses, it is most likely that IVM binds to a similar position in the TM region as in GluCl or GlyR (Estrada-Mondragon & Lynch, 2015; Westergard *et al.* 2015). According to the results of mutagenesis at Ala291 in the α1 subunit, Met286 in the β2 subunit and

Ser301 in the γ2 subunit (corresponding to Gly281 in GluCl or Ala288 in GlyR), IVM induces different effects when it binds to different subunit interfaces: (1) the binding of IVM to the α1–β2 interface (in an anticlockwise orientation of subunit stoichiometry in a top view from the extracellular side) potentiates the GABA-induced current; (2) the binding of IVM to the γ2–β2 interface induces irreversible activation of the channel; (3) IVM cannot bind to the β2–α1 interface because of the large side chain of Met286 in the β2 subunit (Estrada-Mondragon & Lynch, 2015). Further investigations are needed to obtain more detailed information on the modulation mechanisms of GABA$_A$R by IVM.

In the case of nAChR, the IVM-bound structure also remains to be determined. Application of IVM alone does not activate the nAChR, but it potentiates the ACh-induced current at a concentration of 30 μM (Krause *et al.* 1998). Based on docking analyses and functional studies of rat nAChR α7–mouse 5-HT$_3$A chimeras and mutagenesis experiments (Collins & Millar, 2010), IVM also interacts with the amino acid residues located in the upper region of the TMs. However, the predicted IVM-binding site in the nAChR is most likely to be different from those of other Cys-loop receptors (Lynagh & Lynch, 2012). IVM binds to the intra-subunit cavity between TM1 and TM4 (in the same subunit) (Sattelle *et al.* 2009; Collins & Millar, 2010), and this site is distinct from the IVM-binding site in GluCl, GlyR and GABA$_A$R, which is located in the subunit interface, as described above. Ala225Asp, Gln272Val, Thr456Tyr and Cys459Tyr mutations reduced the IVM potency (Collins & Millar, 2010). Surprisingly, Ser222Met (in TM1), Met253Leu (in TM2) and Ser276Val (in TM3) mutations induced a change of the IVM effect from potentiation to inhibition.

P2X receptors. IVM acts as an allosteric positive modulator of purinergic ATP-gated P2X receptors (seven P2X subunits, P2X$_{1–7}$), especially P2X$_4$ but not P2X$_2$ or P2X$_3$ receptors (Khakh *et al.* 1999). IVM alone does not directly activate the P2X$_4$ receptor but potentiates the amplitude of the ATP-induced current with an EC$_{50}$ of approximately 0.25 μM (Priel & Silberberg, 2004; Gao *et al.* 2015). IVM also potentiates the ATP-induced current of the human P2X$_7$ receptor, but has only a limited effect on the mouse and rat P2X$_7$ receptors

(Norenberg *et al.* 2012). Recent findings suggest that IVM mediates alcohol intake, sensorimotor gating and dopamine-induced motor behaviour through modulation of P2X$_4$ receptors (Bortolato *et al.* 2013; Franklin *et al.* 2014, 2015; Khoja *et al.* 2016). IVM also possesses a potential anti-cancer effect: it kills breast cancer cells through potentiating P2X$_4$/P2X$_7$ signalling (Draganov *et al.* 2015).

The crystal structures of an apo (closed) state and an ATP-bound (open) state of the zebrafish P2X$_4$ receptor have been solved (Kawate *et al.* 2009; Hattori & Gouaux, 2012) (Fig. 3), while the IVM-bound state still remains unknown. A previous study showed that extracellular application of IVM modulates human P2X$_4$ receptors better than when applied from the intracellular side, suggesting that IVM does not interact with the intracellular domains (Priel & Silberberg, 2004). The authors also proposed that there are two separate IVM-binding sites in the extracellular domains of the P2X$_4$ receptor: (1) IVM binds to the high affinity site to increase ATP-induced current by reducing channel desensitization; and (2) IVM binds to the low affinity site to decelerate current deactivation by inducing stabilization of the open state. Based on their subsequent functional analyses of the rat

P2X$_4$–rat P2X$_2$ chimeras and mutants, it was shown that IVM most likely interacts with the TMs of open P2X$_4$ receptors, near the extracellular surface of the plasma membrane (Silberberg *et al.* 2007). This predicted IVM binding site, which is located in the upper region of the TMs (Fig. 3), is similar to those of Cys-loop receptors. By scanning mutagenesis of all amino acid residues of TM1 and TM2 to Ala or Trp, it was observed that mutations of Val28, Ile39, Tyr42, Val43 and Val47 in TM1 and Gly340, Gly342, Leu345 and Val348 in TM2 lowered IVM occupancy (Silberberg *et al.* 2007). Other studies also indicated that Gln36, Leu40, Val43, Trp46, Val47 and Trp50 in TM1 and Asn338, Gly342, Leu346, Ala349 and Ile356 in TM2 contribute to the IVM effect (Jelinkova *et al.* 2008; Popova *et al.* 2013). Taken together, the residues in TMs near the extracellular surface of the plasma membrane are critical for IVM action.

Recently, functional studies identified a novel structural determinant of the rat P2X$_4$ receptor for IVM sensitivity, the lateral fenestration (Kawate *et al.* 2009) (Fig. 3), which acts as a linker to connect the extracellular domains and the pore-forming TMs (Rokic *et al.* 2013; Gao *et al.* 2015). Several aromatic residues (Tyr195, Phe198, Phe200 and Phe330) located in the lateral fenestration contribute to
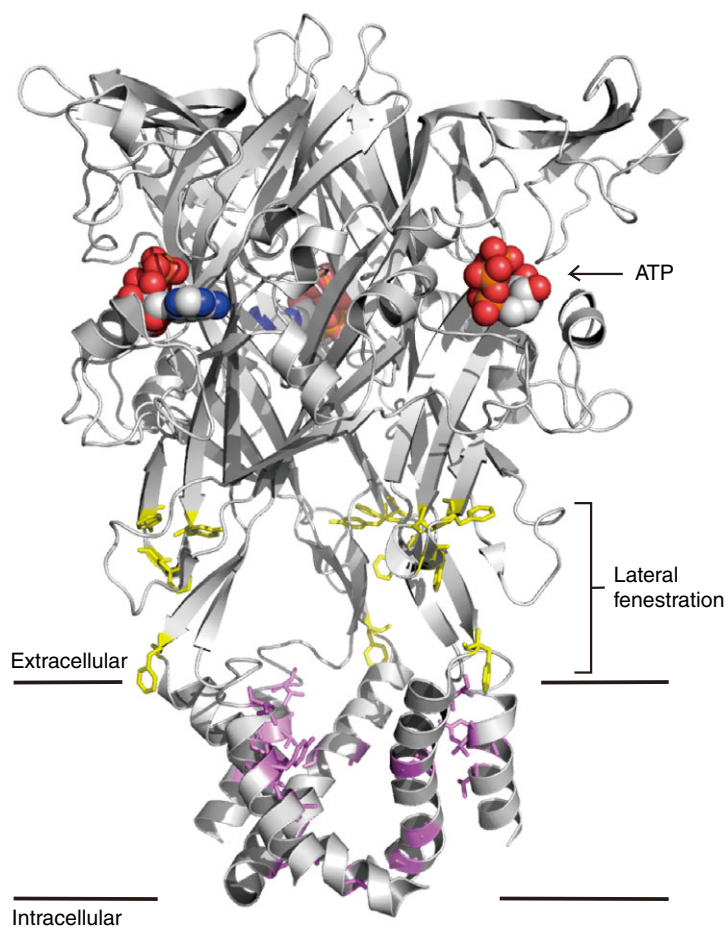
Figure 3. Critical amino acid residues for the IVM effect and the predicted binding site in the P2X$_4$ receptor
A lateral view of the structure of the ATP-bound (open) state zebrafish P2X$_4$ receptor (PDB ID: 4DW1) (Hattori & Gouaux, 2012) trimer. The structure of the IVM-bound P2X$_4$ receptor is still unsolved. ATPs that bind to the extracellular domains are shown in sphere mode. The amino acid residues of the rat P2X$_4$ receptor, which contribute to the IVM response, located in the TMs (violet) and lateral fenestration (yellow), are shown in their corresponding positions in the zebrafish P2X$_4$ structure. The violet residues (TM regions) are the predicted IVM-binding sites, and the yellow residues (lateral fenestration regions) also contribute to the IVM response.

IVM sensitivity and thus modulate current deactivation (Gao *et al.* 2015). A specific negatively charged residue in the human P2X$_4$ receptor, Glu51, located on the top of the extracellular entrance of the channel pore, is also critical for the IVM effect (Samways *et al.* 2012).

G-protein-gated inwardly rectifying K$^+$ channels. IVM acts as a novel activator of GIRK channels (Su *et al.* 2016; Chen *et al.* 2017). GIRK channels (four GIRK subunits, Kir3.1–4) control various physiological functions: Kir3.1–Kir3.2 heterotetramers in the brain regulate the excitability of neurons and Kir3.1–Kir3.4 heterotetramers in the heart regulate heart rate (Kubo *et al.* 1993; Krapivinsky *et al.* 1995; Hibino *et al.* 2010). GIRK channels are known to be directly activated by G$_{\beta\gamma}$ and also directly modulated by phosphatidylinositol 4,5-bisphosphate (PIP$_2$) and Na$^+$ (Logothetis *et al.* 1987; Reuveny *et al.* 1994; Huang *et al.* 1998; Ho & Murrell-Lagnado, 1999). We recently observed that IVM activates Kir3.1–Kir3.2 remarkably (EC$_{50}$ of 3.5 μM) and Kir3.1–Kir3.4 weakly (EC$_{50}$ of 7.5 μM) in a PIP$_2$-dependent, G$_{\beta\gamma}$-independent manner, and identified the structural determinants for IVM-mediated activation (Chen *et al.* 2017).

The crystal structures of the mouse Kir3.2 in an apo (Arg201Ala, closed) state, a PIP$_2$-bound (closed) state (Fig. 4*A*) and a G$_{\beta\gamma}$-bound (pre-open) state have been solved (Whorton & MacKinnon, 2011, 2013), while the full open state is still unknown, and no complexes with IVM have been solved. Based on our observation that IVM activates Kir3.2 more efficiently than Kir3.4 (Fig. 4*B* and *C*), we identified the structural determinants by constructing Kir3.2–Kir3.4 chimeras and single-point mutants (Chen *et al.* 2017). We found that the TMs are not responsible for IVM-mediated GIRK activation, in remarkable contrast to IVM activation in Cys-loop receptors and the P2X$_4$ receptor. A single amino acid residue in Kir3.2, Ile82, located in the slide helix at the end of the N-terminus cytoplasmic region, is critical for the IVM response (Fig. 4*A*). Mutation of Kir3.2 Ile82 (corresponding to Kir3.4 Leu77) to Leu reduced IVM-induced current, and the reverse mutation of Kir3.4 Leu77 (corresponding to Kir3.2 Ile82) to Ile increased the IVM effect. Ile82 is oriented with a methyl group of the branched side chain toward the inner transmembrane helix (TM2), and this methyl group acts as a switch for IVM-mediated activation. Trp91Ala and Ile195Ala mutations also reduced GIRK current induced by IVM, suggesting that Ile82, Trp91 and Ile195, located in the interface between the TMs and the cytoplasmic tail domains (CTDs), determine IVM-mediated GIRK activation, presumably by forming an IVM-binding pocket (Fig. 4*D* and *E*). We speculated that, when IVM binds to the pocket, hydrophobic interactions are induced between IVM and Ile82/Trp91/Ile195, which reinforce

the hydrophobic core around the TM–CTD interface, stabilizing the open state of GIRK channel. Since the PIP$_2$-binding site is close to the pocket formed by Ile82/Trp91/Ile195, the association of PIP$_2$ may support IVM binding by inducing stabilization of the TM–CTD interface (Chen *et al.* 2017).

Farnesoid X receptors. IVM acts as a novel ligand of FXR (Jin *et al.* 2013), a receptor in the cytoplasm belonging to the nuclear hormone receptor superfamily. One of the physiological ligands of FXR is bile acid. It is highly expressed in liver, small intestine, kidney and adrenals (Wang *et al.* 2008). When a ligand binds to FXR, it targets to the DNA and regulates the expression of genes that are involved in the metabolism of bile acids, lipid and glucose (Wang *et al.* 2008). Therefore, the novel FXR ligand, IVM, has a potential to treat metabolic syndromes, such as non-alcoholic fatty liver disease (Wang *et al.* 2008; Jin *et al.* 2013, 2015; Zheng *et al.* 2017). IVM shows a higher FXR selectivity and affinity (EC$_{50}$ of approximately 0.2 μM) than the physiological FXR ligand, bile acid (EC$_{50}$ of approximately 10 μM) (Jin *et al.* 2013; Ding *et al.* 2015).

The crystal structure of the ligand-binding domain of IVM-bound human FXR has been solved (Akwabi-Ameyaw *et al.* 2009; Jin *et al.* 2013) (Fig. 5*A*). The conformational change of the ligand-binding pocket induced by IVM was different from that induced by a widely used FXR ligand, GW4064. The analyses of the transcriptional activity of FXR mutants revealed several important residues for IVM binding (Jin *et al.* 2013, 2015) (Fig. 5*B*). The Ala291Trp mutation reduces the size of the ligand-binding pocket, thereby preventing the binding of FXR ligands (IVM, IVM analogues or GW4064), as well as the transcriptional activity induced by these ligands. The Asn283Leu and Phe284His mutations of FXR abolished the transcriptional activity induced by IVM by disrupting a hydrogen bond between IVM and Asn283, and a hydrophobic interaction between IVM and the hydrophobic side chain of Phe284. Surprisingly, these mutants were still able to be activated by GW4064. On the other hand, Leu287Thr, Arg331Met and His447Phe mutations increased IVM (or its analogues)-activated transcriptional activity, while abolishing the GW4064 effect. It is most likely that these amino acid residues play important roles in the ligand selectivity of FXR.

Comparison of the effects of IVM analogues on target proteins

There are several IVM analogues known to modulate ion channels and receptors like IVM does. These compounds, including abamectin (ABM), doramectin (DOM), eprinomectin (EPM) and emamectin (EMM), share a backbone of a 16-membered macrocyclic lactone
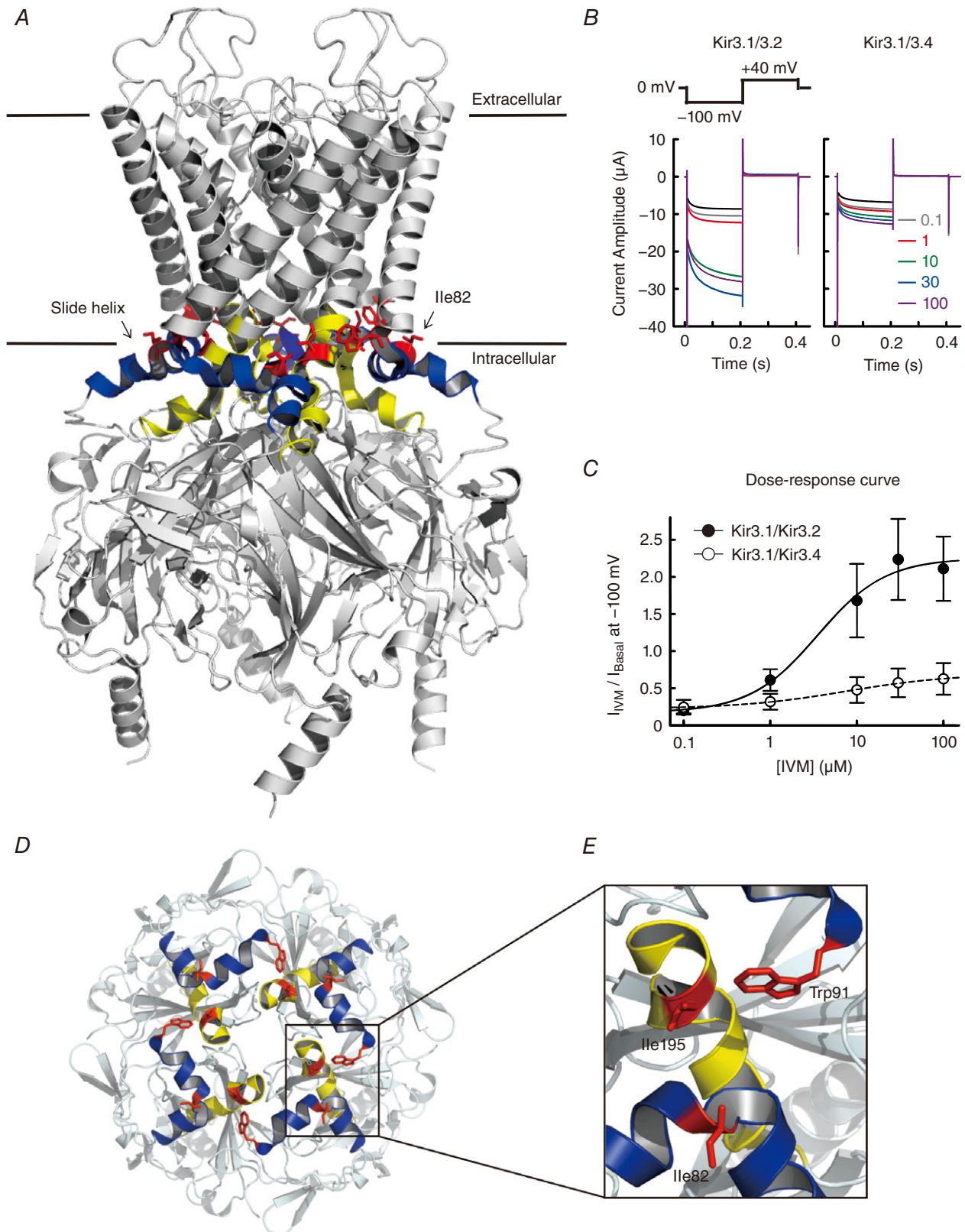
Figure 4. Critical amino acid residues for the IVM effect and the predicted binding site in GIRK channels
A, a lateral view of the structure of the PIP$_2$-bound (closed) state mouse Kir3.2 (PDB ID: 3SYA) (Whorton & MacKinnon, 2011) tetramer. The structure of the IVM-bound GIRK channel is still unsolved. The slide helices are

shown in blue; TM-CTD linkers are shown in yellow; Ile82, Trp91 and Ile195 (the amino acid residues contributing to the IVM response) are shown in red. *B*, currents in the absence (black trace) and presence of IVM ($0.1-100$ μM, coloured traces) in oocytes expressing Kir3.1−Kir3.2 (left) and Kir3.1−Kir3.4 (right) were recorded using the protocol shown above (modified from Fig. 1*A* of Chen *et al.* 2017). *C*, dose–response curves for Kir3.1−Kir3.2 (filled circles) and Kir3.1−Kir3.4 (open circles) were constructed by the ratio of I_{Basal} and I_{IVM}, where I_{Basal} refers to the basal current before the application of IVM, I_{IVM} refers to the maximum current in the presence of IVM at a given concentration at -100 mV, and the basal current was subtracted (modified from Fig. 1*D* of Chen *et al.* 2017). *D*, the top view of the TM–CTD interfaces and intracellular domains of Kir3.2 from the extracellular side. *E*, the expanded view of Ile82, Trp91 and Ile195 located in the TM–CTD interfaces. We speculated that Ile82/Trp91/Ile195 contribute to IVM sensitivity by forming a binding pocket in the TM–CTD interface (Chen *et al.* 2017).

with different functional groups at the benzofuran, spiroketal and disaccharide moieties (Figs 1 and 6*A*). Based on the IVM-bound Cys-loop receptor complexes (Fig. 2), the benzofuran moiety is inserted deeply toward the pore of the channel, the spiroketal moiety interacts with TM1 and the disaccharide moiety orients toward the outside of the channel (Hibbs & Gouaux, 2011; Du *et al.* 2015). In a study that compared the binding of IVM in GluCl and GlyR, it was shown that IVM is inserted deeper into the subunit interfaces in GluCl than in GlyR, supporting the notion that Gly281 in GluCl provides a larger space for IVM binding than Ala288 in GlyR (Huang *et al.* 2017). Therefore, the size of IVM analogues may also influence their binding to target proteins, due to the limited space of the binding pocket.

ABM shares the most similar structure to IVM among these analogues, and their structure differs only at a position between C22 and C23 in the spiroketal moiety (indicated as X–Y in Fig. 6*A*): double bonds in ABM reduced to a single bond in IVM (Omura, 2016). Therefore, ABM induces modulation of most of the target proteins with a similar efficacy to that of IVM. They show equal effects on the activation of GlyR (Lynagh &

Lynch, 2010*b*) and GIRK current (Chen *et al.* 2017), the potentiation of ATP-gated P2X$_4$ current (Silberberg *et al.* 2007) and the regulation of metabolism by modulation of FXR signalling (Jin *et al.* 2015). In the case of the invertebrate GluCl, IVM is most potent and ABM and others are less effective (Arena *et al.* 1995) (Fig. 6*B*).
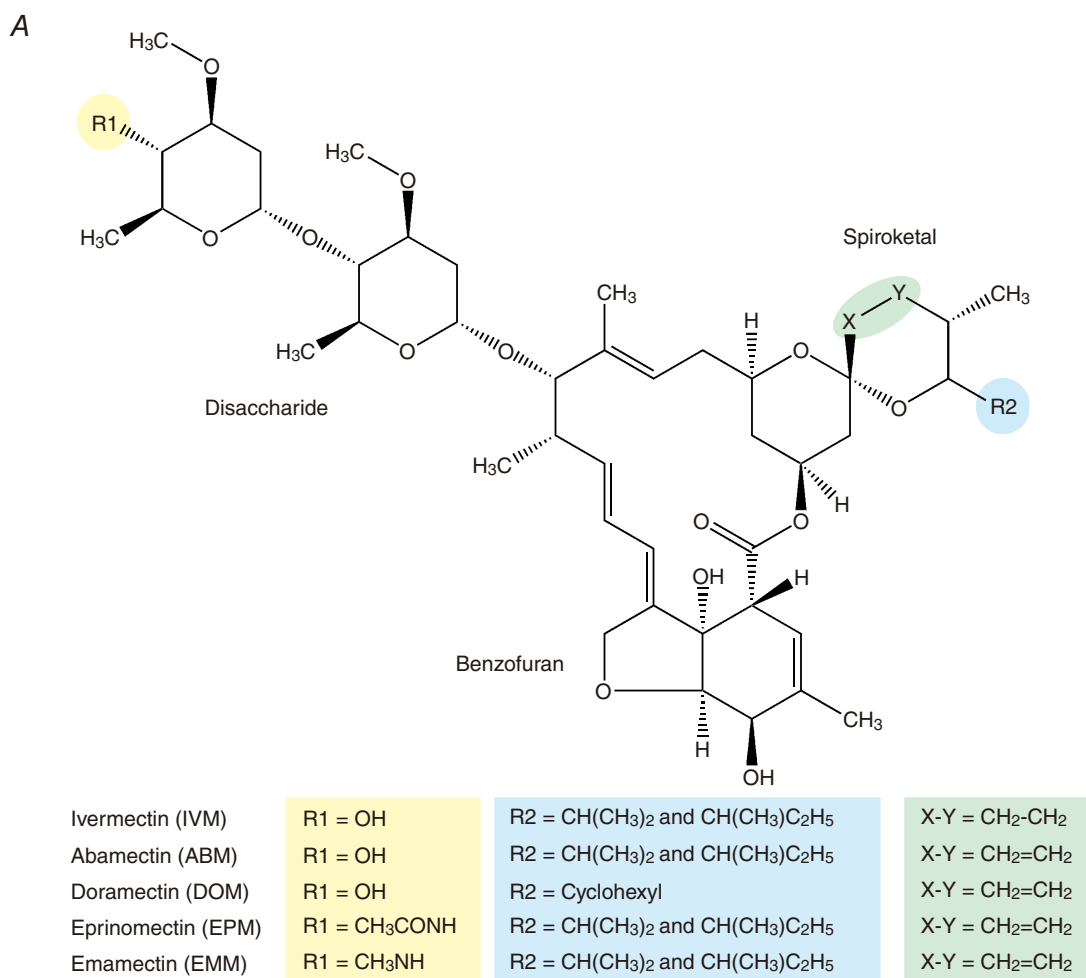
DOM contains a larger functional group in the spiroketal moiety (indicated as R2 in Fig. 6*A*: cyclohexyl). This analogue has less effect on the modulation of P2X$_4$ receptor and GIRK than IVM (Silberberg *et al.* 2007; Chen *et al.* 2017), while it has similar effects on that of Cys-loop receptors and FXR (Arena *et al.* 1995; Lynagh & Lynch, 2010*b*; Jin *et al.* 2015) (Fig. 6*B*). Therefore, we speculate that the IVM-binding space in P2X$_4$ and GIRK may be narrower than that in Cys-loop receptors and FXR.

EPM and EMM contain a larger functional group in the disaccharide moiety (indicated as R1 in Fig. 6*A*). These two analogues have weaker effects on most of the target proteins than IVM (see detail in Fig. 6*B*). For example, EPM did not rescue the metabolic syndrome by targeting FXR (Jin *et al.* 2015). These results suggest that the structural difference in disaccharide moiety also influences its binding.
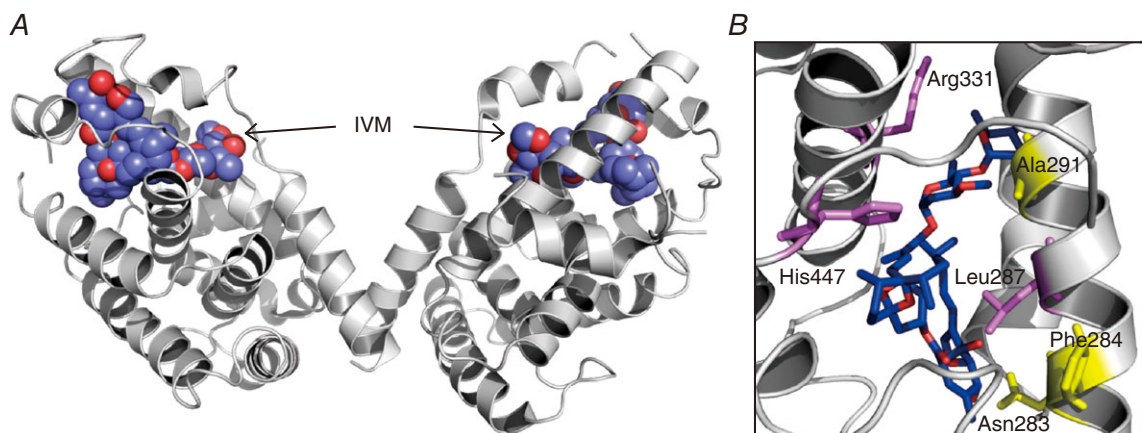
Figure 5. IVM-binding site and structural determinants for binding in FXR
A, the structure of the IVM-bound human FXR ligand-binding domain (PDB ID: 4WVD) (Jin *et al.* 2013) as a dimer. The IVM molecules are shown in sphere mode. The binding of IVM activates FXR and thus regulates the expression of FXR-targeted genes. *B*, the expanded view of the IVM binding site in FXR. Mutations in Asn283, Phe284 and Ala291 (yellow) abolish the IVM response, whereas mutations in Leu287, Arg331 and His447 (violet) increase the IVM response.

A

Ivermectin (IVM)	R1 = OH	R2 = CH(CH$_3$)$_2$ and CH(CH$_3$)C$_2$H$_5$	X-Y = CH$_2$-CH$_2$
Abamectin (ABM)	R1 = OH	R2 = CH(CH$_3$)$_2$ and CH(CH$_3$)C$_2$H$_5$	X-Y = CH$_2$=CH$_2$
Doramectin (DOM)	R1 = OH	R2 = Cyclohexyl	X-Y = CH$_2$=CH$_2$
Eprinomectin (EPM)	R1 = CH$_3$CONH	R2 = CH(CH$_3$)$_2$ and CH(CH$_3$)C$_2$H$_5$	X-Y = CH$_2$=CH$_2$
Emamectin (EMM)	R1 = CH$_3$NH	R2 = CH(CH$_3$)$_2$ and CH(CH$_3$)C$_2$H$_5$	X-Y = CH$_2$=CH$_2$

B   Comparison of the modulation effects of IVM analogues on target proteins

Target proteins	Modulation effects of IVM analogues	References
GluCl	IVM > other analogues	Arena *et al.*, 1995
GlyR	IVM = ABM = DOM = EMM > EPM	Lynagh & Lynch, 2010
P2X4	IVM = ABM >> DOM > EMM	Silberberg *et al.*, 2007
GIRK	IVM = ABM > DOM = EPM	Chen *et al.*, 2017
FXR	IVM = ABM = DOM >>> EPM	Jin *et al.*, 2015

Figure 6. Comparison of chemical structures and effects of IVM analogues on target proteins
A, chemical structures of ivermectin (IVM) and its analogues: abamectin (ABM), doramectin (DOM), eprinomectin (EPM) and emamectin (EMM). *B*, a comparison of the effects of IVM analogues on modulation of the function of target proteins: GluCl (Arena *et al.* 1995), GlyR (Lynagh & Lynch, 2010*b*), P2X$_4$ receptor (Silberberg *et al.* 2007), GIRK (Kir3.1–Kir3.2) channel (Chen *et al.* 2017) and FXR (Jin *et al.* 2015). IVM is the most potent among the analogues to activate GluCl; ABM possesses a similar efficacy to IVM in the activation of GlyR, the P2X$_4$ receptor, GIRK channels and FXR; DOM shows a lesser activation or potentiation effect on the P2X$_4$ receptor and GIRK channels than IVM; EPM does not modulate FXR-mediated signalling.

Summary

Since IVM is such a big and hydrophobic compound, the size of the binding cavity between the α-helices of the TMs or the binding domains generally governs IVM binding. Some of the amino acid residues, whose side chains are oriented to the binding cavity, stabilize IVM binding by forming a hydrophobic interaction and hydrogen bond network.

IVM modulates various ion channels and receptors by different mechanisms: (1) IVM binds to the TMs of Cys-loop receptors near the extracellular surface of the plasma membrane and induces the rotation of TMs, thereby facilitating opening of the channel pore. A small amino acid residue located in TM3 (such as Gly281 in GluCl and Ala288 in GlyR) plays a key role in IVM sensitivity (Fig. 2*D*). (2) IVM most likely interacts with the TMs of the P2X$_4$ receptor by binding to the sub-unit interfaces, and this is similar to the IVM binding site in most of the Cys-loop receptors (Fig. 3). (3) Unlike in Cys-loop receptors and the P2X$_4$ receptor, the TMs of GIRK channels are not critical for the IVM response. We found that the hydrophobic side chain of Ile82 (Kir3.2) at the slide helix, which is located in the interface between the TMs and intracellular domains, is critical for IVM sensitivity (Fig. 4*A*, *D* and *E*). (4) IVM not only embeds into lipid bilayers and then influences the functions of membrane proteins, but also presumably permeates through the membrane and then interacts with the nuclear receptor FXR (Fig. 5).

IVM shows higher affinity to GluCl, P2X$_4$ and FXR (EC$_{50}$ $\leq$ 0.25 μM) than to other targeted channels (EC$_{50}$ 1−10 μM). Therefore, the application of IVM to the treatment of parasitic infections, cancers and metabolic syndrome, through modulation of GluCl-, P2X$_4$- and FXR-mediated signalling, is considered to be saved from side effects due to the modulation of other targets by IVM. On the other hand, since IVM analogues possess a relatively low efficiency compared to IVM toward a specific receptor (Fig. 6*B*), it will be possible to reduce an undesirable influence due to the activation of a specific receptor by replacing IVM with a suitable analogue. Further research is awaited to advance our knowledge of this multifaceted drug, IVM, and its analogues.

References

Adelsberger H, Lepier A & Dudel J (2000). Activation of rat recombinant $\alpha_1\beta_2\gamma_{2S}$ GABA$_A$ receptor by the insecticide ivermectin. *Eur J Pharmacol* **394**, 163–170.

Akwabi-Ameyaw A, Bass JY, Caldwell RD, Caravella JA, Chen L, Creech KL, Deaton DN, Madauss KP, Marr HB, McFadyen RB, Miller AB, Navas F 3rd, Parks DJ, Spearing PK, Todd D, Williams SP & Bruce Wisely G (2009). FXR agonist activity of conformationally constrained analogs of GW 4064. *Bioorg Med Chem Lett* **19**, 4733–4739.

Althoff T, Hibbs RE, Banerjee S & Gouaux E (2014). X-ray structures of GluCl in apo states reveal a gating mechanism of Cys-loop receptors. *Nature* **512**, 333–337.

Arena JP, Liu KK, Paress PS, Frazier EG, Cully DF, Mrozik H & Schaeffer JM (1995). The mechanism of action of avermectins in *Caenorhabditis elegans*: correlation between activation of glutamate-sensitive chloride current, membrane binding, and biological activity. *J Parasitol* **81**, 286–294.

Bortolato M, Yardley MM, Khoja S, Godar SC, Asatryan L, Finn DA, Alkana RL, Louie SG & Davies DL (2013). Pharmacological insights into the role of P2X4 receptors in behavioural regulation: lessons from ivermectin. *Int J Neuropsychopharmacol* **16**, 1059–1070.

Burg RW, Miller BM, Baker EE, Birnbaum J, Currie SA, Hartman R, Kong YL, Monaghan RL, Olson G, Putter I, Tunac JB, Wallick H, Stapley EO, Oiwa R & Omura S (1979). Avermectins, new family of potent anthelmintic agents: producing organism and fermentation. *Antimicrob Agents Chemother* **15**, 361–367.

Calimet N, Simoes M, Changeux JP, Karplus M, Taly A & Cecchini M (2013). A gating mechanism of pentameric ligand-gated ion channels. *Proc Natl Acad Sci USA* **110**, E3987–E3996.

Campbell WC & Benz GW (1984). Ivermectin: a review of efficacy and safety. *J Vet Pharmacol Ther* **7**, 1–16.

Campbell WC, Fisher MH, Stapley EO, Albers-Schonberg G & Jacob TA (1983). Ivermectin: a potent new antiparasitic agent. *Science* **221**, 823–828.

Chabala JC, Mrozik H, Tolman RL, Eskola P, Lusi A, Peterson LH, Woods MF, Fisher MH, Campbell WC, Egerton JR & Ostlind DA (1980). Ivermectin, a new broad-spectrum antiparasitic agent. *J Med Chem* **23**, 1134–1136.

Chen IS, Tateyama M, Fukata Y, Uesugi M & Kubo Y (2017). Ivermectin activates GIRK channels in a PIP$_2$-dependent, G$_{\beta\gamma}$-independent manner and an amino acid residue at the slide helix governs the activation. *J Physiol* **595**, 5895–5912.

Collins T & Millar NS (2010). Nicotinic acetylcholine receptor transmembrane mutations convert ivermectin from a positive to a negative allosteric modulator. *Mol Pharmacol* **78**, 198–204.

Cully DF, Vassilatis DK, Liu KK, Paress PS, Van der Ploeg LH, Schaeffer JM & Arena JP (1994). Cloning of an avermectin-sensitive glutamate-gated chloride channel from *Caenorhabditis elegans*. *Nature* **371**, 707–711.

Ding L, Yang L, Wang Z & Huang W (2015). Bile acid nuclear receptor FXR and digestive system diseases. *Acta Pharmaceutica Sinica B* **5**, 135–144.

Draganov D, Gopalakrishna-Pillai S, Chen YR, Zuckerman N, Moeller S, Wang C, Ann D & Lee PP (2015). Modulation of P2X4/P2X7/Pannexin-1 sensitivity to extracellular ATP via Ivermectin induces a non-apoptotic and inflammatory form of cancer cell death. *Sci Rep* **5**, 16222.

Du J, Lu W, Wu S, Cheng Y & Gouaux E (2015). Glycine receptor mechanism elucidated by electron cryo-microscopy. *Nature* **526**, 224–229.

Egerton JR, Ostlind DA, Blair LS, Eary CH, Suhayda D, Cifelli S, Riek RF & Campbell WC (1979). Avermectins, new family of potent anthelmintic agents: efficacy of the B1a component. *Antimicrob Agents Chemother* **15**, 372–378.

Estrada-Mondragon A & Lynch JW (2015). Functional characterization of ivermectin binding sites in $\alpha 1\beta 2\gamma 2L$ GABA$_A$ receptors. *Front Mol Neurosci* **8**, 55.

Franklin KM, Asatryan L, Jakowec MW, Trudell JR, Bell RL & Davies DL (2014). P2X4 receptors (P2X4Rs) represent a novel target for the development of drugs to prevent and/or treat alcohol use disorders. *Front Neurosci* **8**, 176.

Franklin KM, Hauser SR, Lasek AW, Bell RL & McBride WJ (2015). Involvement of purinergic P2X4 receptors in alcohol intake of high-alcohol-drinking (HAD) rats. *Alcohol Clin Exp Res* **39**, 2022–2031.

Gao C, Yu Q, Xu H, Zhang L, Liu J, Jie Y, Ma W, Samways DS & Li Z (2015). Roles of the lateral fenestration residues of the P2X$_4$ receptor that contribute to the channel function and the deactivation effect of ivermectin. *Purinergic Signal* **11**, 229–238.

Ghosh R, Andersen EC, Shapiro JA, Gerke JP & Kruglyak L (2012). Natural variation in a chloride channel subunit confers avermectin resistance in *C. elegans*. *Science* **335**, 574–578.

Hattori M & Gouaux E (2012). Molecular mechanism of ATP binding and ion channel activation in P2X receptors. *Nature* **485**, 207–212.

Hibbs RE & Gouaux E (2011). Principles of activation and permeation in an anion-selective Cys-loop receptor. *Nature* **474**, 54–60.

Hibino H, Inanobe A, Furutani K, Murakami S, Findlay I & Kurachi Y (2010). Inwardly rectifying potassium channels: their structure, function, and physiological roles. *Physiol Rev* **90**, 291–366.

Ho IH & Murrell-Lagnado RD (1999). Molecular mechanism for sodium-dependent activation of G protein-gated K$^+$ channels. *J Physiol* **520**, 645–651.

Huang CL, Feng S & Hilgemann DW (1998). Direct activation of inward rectifier potassium channels by PIP$_2$ and its stabilization by G$\beta\gamma$. *Nature* **391**, 803–806.

Huang X, Chen H & Shaffer PL (2017). Crystal structures of human GlyRα3 bound to ivermectin. *Structure* **25**, 945–950.e2.

Jelinkova I, Vavra V, Jindrichova M, Obsil T, Zemkova HW, Zemkova H & Stojilkovic SS (2008). Identification of P2X$_4$ receptor transmembrane residues contributing to channel gating and interaction with ivermectin. *Pflugers Arch* **456**, 939–950.

Jin L, Feng X, Rong H, Pan Z, Inaba Y, Qiu L, Zheng W, Lin S, Wang R, Wang Z, Wang S, Liu H, Li S, Xie W & Li Y (2013). The antiparasitic drug ivermectin is a novel FXR ligand that regulates metabolism. *Nat Commun* **4**, 1937.

Jin L, Wang R, Zhu Y, Zheng W, Han Y, Guo F, Ye FB & Li Y (2015). Selective targeting of nuclear receptor FXR by avermectin analogues with therapeutic effects on nonalcoholic fatty liver disease. *Sci Rep* **5**, 17288.

Kane NS, Hirschberg B, Qian S, Hunt D, Thomas B, Brochu R, Ludmerer SW, Zheng Y, Smith M, Arena JP, Cohen CJ, Schmatz D, Warmke J & Cully DF (2000). Drug-resistant *Drosophila* indicate glutamate-gated chloride channels are targets for the antiparasitics nodulisporic acid and ivermectin. *Proc Natl Acad Sci USA* **97**, 13949–13954.

Kauthale RR, Dadarkar SS, Husain R, Karande VV & Gatne MM (2015). Assessment of temperature-induced hERG channel blockade variation by drugs. *J Appl Toxicol* **35**, 799–805.

Kawate T, Michel JC, Birdsong WT & Gouaux E (2009). Crystal structure of the ATP-gated P2X$_4$ ion channel in the closed state. *Nature* **460**, 592–598.

Khakh BS, Proctor WR, Dunwiddie TV, Labarca C & Lester HA (1999). Allosteric control of gating and kinetics at P2X$_4$ receptor channels. *J Neurosci* **19**, 7289–7299.

Khoja S, Shah V, Garcia D, Asatryan L, Jakowec MW & Davies DL (2016). Role of purinergic P2X4 receptors in regulating striatal dopamine homeostasis and dependent behaviors. *J Neurochem* **139**, 134–148.

Krapivinsky G, Gordon EA, Wickman K, Velimirovic B, Krapivinsky L & Clapham DE (1995). The G-protein-gated atrial K$^+$ channel IKACh is a heteromultimer of two inwardly rectifying K$^+$-channel proteins. *Nature* **374**, 135–141.

Krause RM, Buisson B, Bertrand S, Corringer PJ, Galzi JL, Changeux JP & Bertrand D (1998). Ivermectin: a positive allosteric effector of the $\alpha 7$ neuronal nicotinic acetylcholine receptor. *Mol Pharmacol* **53**, 283–294.

Kubo Y, Reuveny E, Slesinger PA, Jan YN & Jan LY (1993). Primary structure and functional expression of a rat G-protein-coupled muscarinic potassium channel. *Nature* **364**, 802–806.

Logothetis DE, Kurachi Y, Galper J, Neer EJ & Clapham DE (1987). The $\beta\gamma$ subunits of GTP-binding proteins activate the muscarinic K$^+$ channel in heart. *Nature* **325**, 321–326.

Lynagh T & Lynch JW (2010*a*). A glycine residue essential for high ivermectin sensitivity in Cys-loop ion channel receptors. *Int J Parasitol* **40**, 1477–1481.

Lynagh T & Lynch JW (2010*b*). An improved ivermectin-activated chloride channel receptor for inhibiting electrical activity in defined neuronal populations. *J Biol Chem* **285**, 14890–14897.

Lynagh T & Lynch JW (2012). Ivermectin binding sites in human and invertebrate Cys-loop receptors. *Trends Pharmacol Sci* **33**, 432–441.

McCavera S, Rogers AT, Yates DM, Woods DJ & Wolstenholme AJ (2009). An ivermectin-sensitive glutamate-gated chloride channel from the parasitic nematode *Haemonchus contortus*. *Mol Pharmacol* **75**, 1347–1355.

Michael B, Meinke PT & Shoop W (2001). Comparison of ivermectin, doramectin, selamectin, and eleven intermediates in a nematode larval development assay. *J Parasitol* **87**, 692–696.

Miller PS & Aricescu AR (2014). Crystal structure of a human GABA$_A$ receptor. *Nature* **512**, 270–275.

Morales-Perez CL, Noviello CM & Hibbs RE (2016). X-ray structure of the human $\alpha 4\beta 2$ nicotinic receptor. *Nature* **538**, 411–415.

Mounsey KE, Dent JA, Holt DC, McCarthy J, Currie BJ & Walton SF (2007). Molecular characterisation of a pH-gated chloride channel from *Sarcoptes scabiei*. *Invert Neurosci* **7**, 149–156.

Nakatani Y, Furutani S, Ihara M & Matsuda K (2016). Ivermectin modulation of pH-sensitive chloride channels in the silkworm larvae of *Bombyx mori*. *Pestic Biochem Physiol* **126**, 1–5.

Norenberg W, Sobottka H, Hempel C, Plotz T, Fischer W, Schmalzing G & Schaefer M (2012). Positive allosteric modulation by ivermectin of human but not murine P2X7 receptors. *Br J Pharmacol* **167**, 48–66.

Omura S (2016). A splendid gift from the earth: The origins and impact of the avermectins (Nobel Lecture). *Angew Chem* **55**, 10190–10209.

Popova M, Trudell J, Li K, Alkana R, Davies D & Asatryan L (2013). Tryptophan 46 is a site for ethanol and ivermectin action in P2X4 receptors. *Purinergic Signal* **9**, 621–632.

Priel A & Silberberg SD (2004). Mechanism of ivermectin facilitation of human P2X4 receptor channels. *J Gen Physiol* **123**, 281–293.

Reuveny E, Slesinger PA, Inglese J, Morales JM, Iniguez-Lluhi JA, Lefkowitz RJ, Bourne HR, Jan YN & Jan LY (1994). Activation of the cloned muscarinic potassium channel by G protein $\beta\gamma$ subunits. *Nature* **370**, 143–146.

Rokic MB, Stojilkovic SS, Vavra V, Kuzyk P, Tvrdonova V & Zemkova H (2013). Multiple roles of the extracellular vestibule amino acid residues in the function of the rat P2X4 receptor. *PLoS One* **8**, e59411.

Samways DS, Khakh BS & Egan TM (2012). Allosteric modulation of Ca^{2+} flux in ligand-gated cation channel (P2X4) by actions on lateral portals. *J Biol Chem* **287**, 7594–7602.

Sattelle DB, Buckingham SD, Akamatsu M, Matsuda K, Pienaar IS, Jones AK, Sattelle BM, Almond A & Blundell CD (2009). Comparative pharmacology and computational modelling yield insights into allosteric modulation of human $\alpha 7$ nicotinic acetylcholine receptors. *Biochem Pharmacol* **78**, 836–843.

Shan Q, Haddrill JL & Lynch JW (2001). Ivermectin, an unconventional agonist of the glycine receptor chloride channel. *J Biol Chem* **276**, 12556–12564.

Sigel E & Steinmann ME (2012). Structure, function, and modulation of GABA_A receptors. *J Biol Chem* **287**, 40224–40231.

Silberberg SD, Li M & Swartz KJ (2007). Ivermectin interaction with transmembrane helices reveals widespread rearrangements during opening of P2X receptor channels. *Neuron* **54**, 263–274.

Su Z, Brown EC, Wang W & MacKinnon R (2016). Novel cell-free high-throughput screening method for pharmacological tools targeting K^+ channels. *Proc Natl Acad Sci USA* **113**, 5748–5753.

Unwin N (2005). Refined structure of the nicotinic acetylcholine receptor at 4A resolution. *J Mol Biol* **346**, 967–989.

Wang YD, Chen WD, Moore DD & Huang W (2008). FXR: a metabolic regulator and cell protector. *Cell Res* **18**, 1087–1095.

Westergard T, Salari R, Martin JV & Brannigan G (2015). Interactions of L-3,5,3′-triiodothyronine [corrected], allopregnanolone, and ivermectin with the GABA_A receptor: evidence for overlapping intersubunit binding modes. *PLoS One* **10**, e0139072.

Whorton MR & MacKinnon R (2011). Crystal structure of the mammalian GIRK2 K^+ channel and gating regulation by G proteins, PIP_2, and sodium. *Cell* **147**, 199–208.

Whorton MR & MacKinnon R (2013). X-ray structure of the mammalian GIRK2–$\beta\gamma$ G-protein complex. *Nature* **498**, 190–197.

Zemkova H, Tvrdonova V, Bhattacharya A & Jindrichova M (2014). Allosteric modulation of ligand gated ion channels by ivermectin. *Physiol Res* **63**(Suppl 1), S215–S224.

Zheng Y, Hirschberg B, Yuan J, Wang AP, Hunt DC, Ludmerer SW, Schmatz DM & Cully DF (2002). Identification of two novel *Drosophila melanogaster* histamine-gated chloride channel subunits expressed in the eye. *J Biol Chem* **277**, 2000–2005.

Zheng Z, Zhao Z, Li S, Lu X, Jiang M, Lin J, An Y, Xie Y, Xu M, Shen W, Guo G, Huang Y, Li S, Zhang X & Xie W (2017). Altenusin, a non-steroidal microbial metabolite, attenuates non-alcoholic fatty liver disease by activating the farnesoid X receptor. *Mol Pharmacol* **92**, 425–436.

Additional information

Competing interests

The authors declare no competing financial interests.

Author contributions

I-S.C. and Y.K. conceived and wrote the review. All authors have approved the final version of the manuscript and agree to be accountable for all aspects of the work. All persons designated as authors qualify for authorship, and all those who qualify for authorship are listed.

Funding

Acknowledgements